Dynamical analysis of the so-called Ziegler column

[redacted]

February 14, 2022

1 Introduction

In this report, we present the study of a dynamical system's stability : the Ziegler column.

This kind of structure can be met in the aerodynamic field with wings equipped of flats or deflectors (in simple flat cases) [1][2]. An issue then is that in addition to divergence (too high loading), the structure may be subject to undamped oscillations resulting into aero flutter [3].

The Ziegler column is a simple model made of two consecutive rods (slender rigid structure) bounded to each other or to the ground by viscous torsion springs:

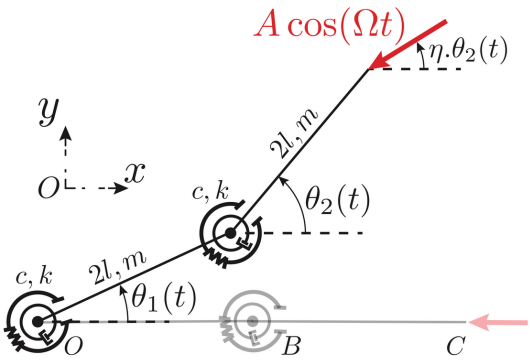

Figure 1: Ziegler column - at rest and deformed

This system obeys to the following non-linear coupled non-dimensionalized differential equations:

$$
\begin{aligned}
0 &= \ddot{\theta}_1 + \frac{3}{8}\ddot{\theta}_2 cos(\theta_1 - \theta_2) \\
&+ \frac{3}{8}\dot{\theta}_2^2 sin(\theta_1 - \theta_2) + \frac{1}{Q}\dot{\theta}_1 - \frac{1}{2Q}\dot{\theta}_2 + \frac{3}{8}\theta_1 - \frac{3}{16}\theta_2 \\
&+ \lambda cos(\beta\tau)\left[cos(\theta_1)sin(\eta\theta_2) - sin(\theta_1)cos(\eta\theta_2)\right]
\end{aligned}
$$

$$
\begin{aligned}
0 &= \ddot{\theta}_2 + \frac{3}{2}\ddot{\theta}_1 cos(\theta_1 - \theta_2) \\
&- \frac{3}{2}\dot{\theta}_1^2 sin(\theta_1 - \theta_2) + \frac{2}{Q}\dot{\theta}_2 - \frac{2}{Q}\dot{\theta}_1 + \frac{3}{4}\theta_2 - \frac{3}{4}\theta_1 \\
&+ 4\lambda cos(\beta\tau)\left[cos(\theta_2)sin(\eta\theta_2) - sin(\theta_2)cos(\eta\theta_2)\right]
\end{aligned}
$$

and it's entirely defined by angles θ_α ($\alpha = 0, 1$), provided one knows variables:

- $\tau = \omega_n.t$ adim time $\omega_n = \sqrt{k/(ml^2)}$;
- $Q = 8k/(3.c.\omega_n)$ damping factor ;
- $\lambda = A/(8k/3l)$ amplitude force ;
- $\beta = \Omega/\omega_n$ pulsation force ;

In this report, we want to characterize equilibrium of the structure under a right hand side force, modelling incoming flow for instance, that one can modulate in several ways:

- λ controls the intensity of forcing term;
- β controls the pulsation of forcing term;
- η controls the direction of forcing term.

Given the system's non-linearity it's convenient to rewrite the differential equations 1 under a more coding-friendly shape A:

$$
\begin{bmatrix} \underline{\underline{\mathbb{O}}} & \underline{\underline{\mathbb{M}}} \\ \underline{\underline{\mathbb{I}}} & \underline{\underline{\mathbb{O}}} \end{bmatrix} \dot{\underline{y}} - \begin{bmatrix} -\underline{\underline{\mathbb{K}}} & -\underline{\underline{\mathbb{C}}} \\ \underline{\underline{\mathbb{O}}} & \underline{\underline{\mathbb{I}}} \end{bmatrix} \underline{y} + \begin{bmatrix} \underline{\mathbb{F}}_{NL} \\ \underline{O} \end{bmatrix} = \underline{0} \qquad (1)
$$

with $\underline{y} = {}^t[\theta_1; \theta_2; \dot{\theta}_1; \dot{\theta}_2]$

Under this form, we can see the system as the combination of dynamic matrices and a non-linear vector. One can then go from non-linear to linear case by linearizing around rest state θ_α=(0, 0) and removing this non-linear vector, such that then $\dot{\underline{y}} = \underline{\underline{J}}.\underline{y}$. It's then easy to go from one formulation to the other one.

Besides, this differential system can now be easily implemented in *odeint* python solver. Finally, in order to give to this report some physical meaning, we will undergo some stability study assuming we aim at answering the following problematic :

For an application to a plane design, we would like to know under which conditions on the force one can avoid low amplitude resonances ?

2 Overview stability system

Let's first and foremost show different behaviors of the structure for different sets of loading (η, β, λ):

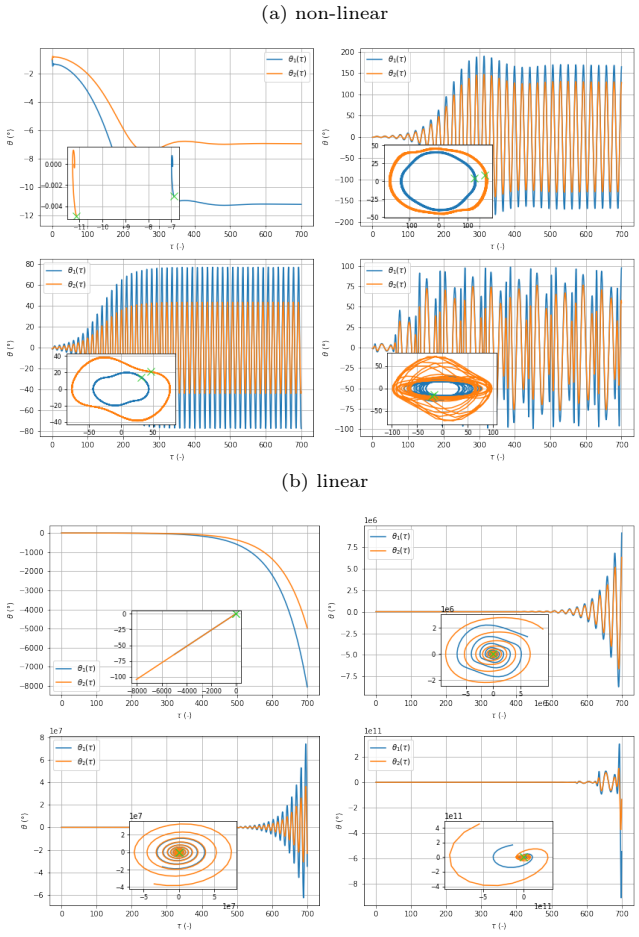

Figure 2: Miscellaneous dynamic behaviors of the system. For both linear and non-linear cases : a) Bifurcation to an equilibrium state for $\eta = 0$, $\beta = 0$ and $\lambda = 0.072$. b) Flip bifurcation to a dynamic state with a $2\bar{T}$-period for $\eta = 0$, $\beta = 0.584$ and $\lambda = 0.036$. c) Hopf bifurcation to a periodic stationary state for $\eta = 1$, $\beta = 0$ and $\lambda = 0.4$. (d) Secondary Hopf or Neimark-Sacker bifurcation on a quasi-periodic state for $\eta = 1$, $\beta = 0.1$ and $\lambda = 0.6$. Insets show the bifurcated stationary states in the state space $(\theta(\tau), \dot{\theta}(\tau))$, as well as initial state with a green cross.

We observe here that the non-linearities one neglects in the linear case in fact account for a part of the system's damping.

However, the **approach** adopted through the paper is meant **to highlight** some **characteristic behaviors** of the system, and to deduce conditions of stability/instability. To this aim, in the following, we will **linearize around** ${}^t[\mathbf{0, 0, 0, 0}]$ position, in the **undamped case** ($C = 0$) and try to characterize dynamic motion form the **linear** problem, while doing the **link** with physical **non-linear** problem.

3 Modulation parameters

We aim at understanding the system's conditions of equilibrium as well as physical links one may do with aforementioned aerodynamic fields.

3.1 Buckling - $\eta = 0$, $\beta = 0$, λ

First, we look at how system is responding from an exterior stimulation, the application of a constant horizontal force. The system can be associated to the buckling of a horizontal bar. As we consider rotation springs in two points of the structure, this change of geometry is studied under stability theory and not from a deformation point of view.

We then expect the system to be able to enter in resonance for specific sets of variables (η, β, λ). We have two approaches : first a mathematical point of view (eigenvalues) and then a physical (bifurcation diagram) point of view:

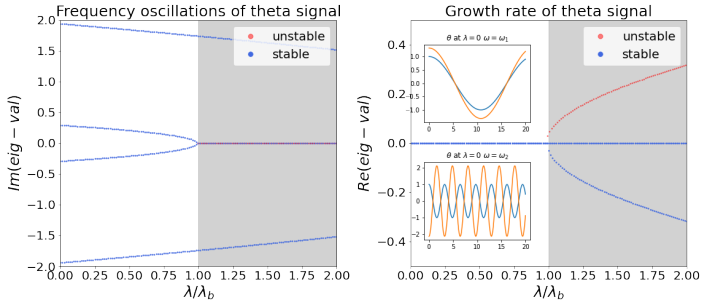

Figure 3: Bifurcation diagram - buckling. a) imaginary part of the eigen values of linear matrix J providing information on oscillating behavior. b) real part of J matrix, telling when system is unstable in function of loading value. Insets provides motion of eigenmodes 1 & 2

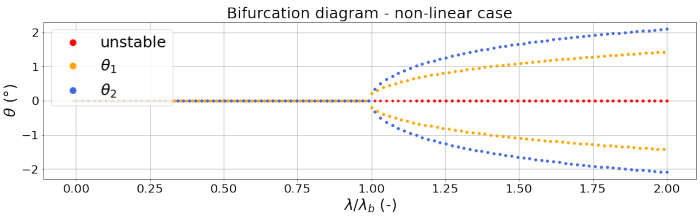

Figure 4: Supercritical Pitchfork bifurcation diagram - non linear case. Non-linear case considered to show equilibrium states associated to fig 3. We are in a supercritical case in non-linear case, but in the subcritical case when in linear case.

In figure 3 we have both real and imaginary part of J's eigenvalues, together with some insight on eigen-modes.

These insets tells us about first and second eigenmodes, that one should combine through a linear system in order to re-build dynamical behavior. The point here is to give an idea of the vibration modes that are encountered in the system, namely in phase ($\omega_1 = 0.29$) and in opposite phase ($\omega_2 = 1.94$) behaviors.

Figure 4 provides associated equilibrium states that one can observe in the non-linear case where energy provided by user through force term leads to new equilibrium states. Eventually, we get 3 different states : to the two stable states of figure 3 are associated the upper and lower branches while to the unstable state is associated position $\theta = 0$ rad.

This can be rephrased as : the system remains at equilibrium (marginally or asymptotically stable) until we reach limit load $\lambda_b \approx 0.072$ above which a simple offset from rest state leads to a new equilibrium state in the non-linear case, and instability in the linear case.

This brings some questions such as

- what is the dynamic motion of the system as a function of loading ?
- what changes in dynamic motion depending on λ value? on Q value ?

Dynamic behavior

We try to tackle the questions of system's motion across time:

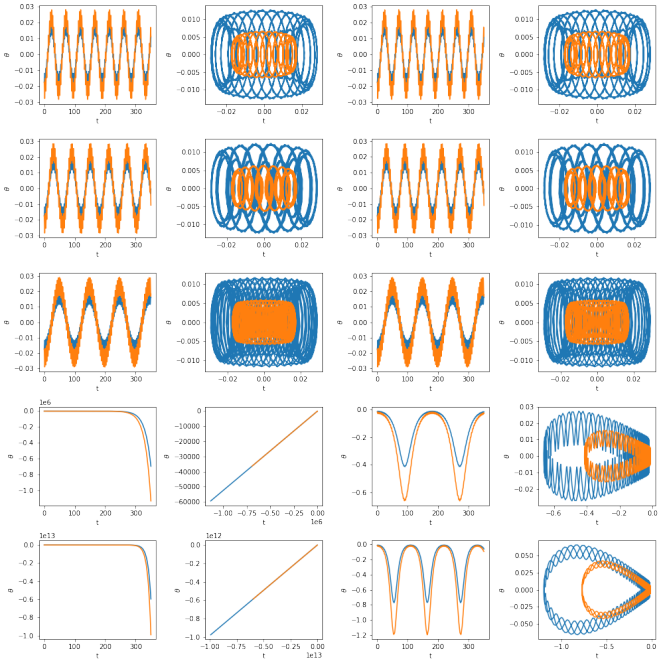

Figure 5: Dynamic behavior - theta in radiant

It comes from figure 5 that linear and non-linear equations share same dynamic behavior as long as angles θ_{alpha} remain low.

The difference comes once we are at $\lambda > \lambda_b$ where non-linear case remains stable while linear case doesn't. This confirm the observation previously made : terms neglected in non-linear case account for some of the system's damping.

We then note that system's behavior depends a lot on damping in the structure. In practical terms, depending on the value of C, the system can either be : marginally stable (e.g. undamped case at $\lambda < \lambda_b$), asymptotically stable (e.g. damped case at $\lambda < \lambda_b$, or unstable (e.g. flutter load).

Physically, asymptotic stability is closer to real damped case while marginal stability is the perfect not-much encountered undamped case. Once again, we consider this last case in the study to observe characteristic behavior of the structure.

We will develop furthermore these questions in the next part, where we will extend our study to another case, the non-conservative case $\eta = 1$.

3.2 Non conservative force - $\eta = 1$, $\beta = 0$, λ

We now consider the case of a non-conservative compression force which is in direction of θ_2 (still constant of time).

A linearization of the differential system around the natural equilibrium point ${}^t[0, 0, 0, 0]$ allows one to study the response of the system around this point. A modal analysis shows the stable and unstable states as a function of the applied non-dimensional load:

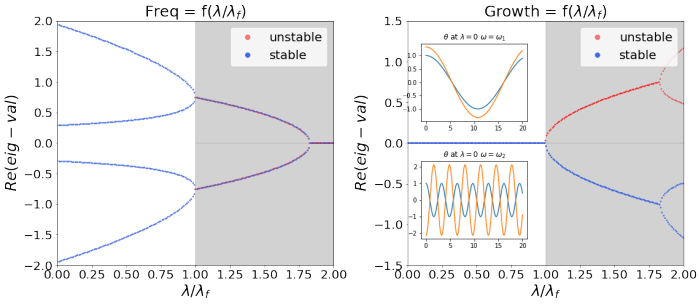

Figure 6: Modal diagram of the system - non conservative compression force

This case is closer in modelisation to the aforementioned airfoil with flap case (except we don't consider deformation). For instance, the aeroelasticity field gather the study of aerodynamic structures for which incoming flow has a direct effect on the structure. Then, the incoming force and structure are bounded such that dynamic motion depends on flow, deformation, etc. One can then talk about aeroelastic problem where we usually study divergence or flutter speed.

While divergence speed is the speed at which there is breaking of the wing under a too high forcing (static instability [4]), the flutter speed is closer in meaning to what we study here. We talk about flutter and not divergence as the system gets unstable by the growth of oscillations.

According to figure 6 we see that flutter takes place when real part of J matrix's eigenvalues is positive, namely only when the load is greater than the critical value $\lambda_f \approx 0.47$. If one applies a smaller force, then the real part of the Jacobian's eigenvalues is zero and so the response is stable.

On a physical point of view, one can think in terms of bifurcation diagram. To this aim the maximum amplitude of the system response has been plotted as a function of the λ/λ_f ratio. For a value of $Q = 10$ it came:

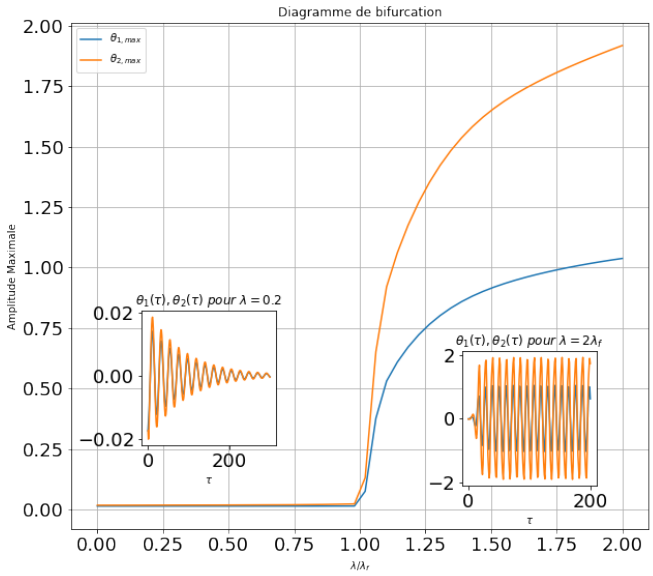

Figure 7: Supercritical Pitchfork bifurcation diagram - non conservative case. Figure shows equilibrium states in the damped non-linear case.

When plotting the bifurcation diagram, it appeared that damping factor Q influences a lot first critical flutter load λ_f.

Solving the differential system for different damping coefficient Q brought that the dependence of λ_f on Q is such that the critical load tends to infinity when $Q \to 0$ then decreases to its minimum around the value of $Q = 15$ with $\lambda_f = 0.31$ and then increases to the asymptotic value of $\lambda_f = 0.47$ when $Q \to \infty$.

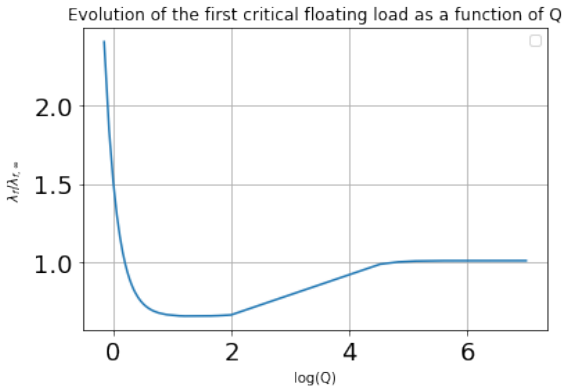

Figure 8: Evolution of the first critical flutter load with Q

For one to consider or not damping therefore radically changes the dynamic of the system. That means graph 8 shows a qualitative behavior of the system in the non-linear case, that one should put in perspective with value of damping coefficient.

To sum up, we now know our system can be a simple model in the study of aerodynamic structures and we furthermore know that flutter will occur above critical load λ_f, while structure's motions is made of stable or unstable oscillations, depending on what parametrization one chooses (i.e. what values of η, λ, Q, ...).

In addition to loading, the pulsation has a great effect on stability, let's develop this point.

3.3 Periodic force - $\eta = 0$, β, $\lambda = 0.75.\lambda_b$

We no longer consider a constant load but rather a time dependent one. In simple terms, we here alternatively apply compression and traction to the Ziegler column. Then, depending on the force we apply and when we apply it, it's possible that the system will either stabilize across time or on the contrary diverge from equilibrium state (0,0). When working on such a system, studying its stability becomes much harsher. However, a way of studying it appears when one considers a periodic system. One can then use what is known as Floquet theory.

The method is similar to the one we used so far : we look at solution's growth or decay along time without looking at the solution itself. The difference stands in the fact we here look at evolution across one period only:

$$\begin{aligned} & \dot{\underline{y}}(t) = \underline{\underline{J}}(t).\underline{y}(t) \\ \to \quad & \dot{\underline{y}}(t+T) = \underline{\underline{J}}(t+T).\underline{y}(t+T) \\ \to \quad & \dot{\underline{y}}(t+T) = \underline{\underline{J}}(t).\underline{y}(t+T) \end{aligned}$$

By looking at stability along 1 period, we can then extrapolate for $t \to \infty$. To do so, we use 4 unit initial vectors : ${}^t[1,0,0,0]$, ${}^t[0,1,0,0]$, ${}^t[0,0,1,0]$, ${}^t[0,0,0,1]$. We implement these in above system and it leads to 4 vectors at $t+T$. The point then is to combine these states after period T to build what is known as the monodromy matrix ϕ. Eventually, the eigenvalues σ_i of this matrix (i.e. Floquet multipliers) tells if motion will be stable or unstable :

- $|\sigma_i| < 1 \Rightarrow$ the solution is stable ;
- $|\sigma_i| > 1 \Rightarrow$ the solution is unstable ;

Decomposing these Floquet multipliers into a real part and an imaginary part, we have equivalently [5] :

$$\begin{aligned} & \sigma_i = \rho_i.e^{j.\kappa_i} \\ \to \quad & f_i = \frac{log(\rho_i)}{T} + j.\frac{\kappa_i \pm 2k\pi}{T} = \frac{log(\rho_i)}{T} + j.\left(\frac{\kappa_i}{T} \pm k.\beta\right) \end{aligned}$$

with $k \in \mathbb{N}$ and where stability now reads

- $|Re(f_i)| > 0 \Rightarrow$ the solution is unstable ;
- $|Re(f_i)| < 0 \Rightarrow$ the solution is stable ;

Plotting the real and imaginary part of Floquet exponent f_i, we get for the set ($\eta = 0$, $\lambda = 0.75.\lambda_b$, β) the following results:

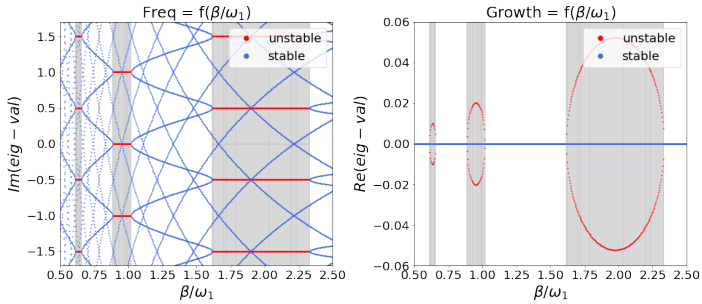

Figure 9: Modal diagram of the system - periodic compression force

From figure 9 we can see that instability occurs in specific zones only. By normalizing pulsation with respect to lower eigenfrequency $\omega_1 \approx 0.29$, we then see that the system resonates when force is modulated at a multiple of eigenfrequencies. Generally speaking, if one was considering a larger scale for β we would observe some vibrations associated to 2nd eigenfrequency ω_2.

The lhs figure shows imaginary part of Floquet multipliers, periodized every β, thus providing frequencies at which structure vibrates. It appears then that when structure is unstable it explodes while oscillating, namely flutter is observed.

Let's generalize our observation by looking to both parameters λ and β and their influence on instability.

4 Instability tongues

We here extend Floquet theory to the mapping of instability in function of both amplitude λ and pulsation β:

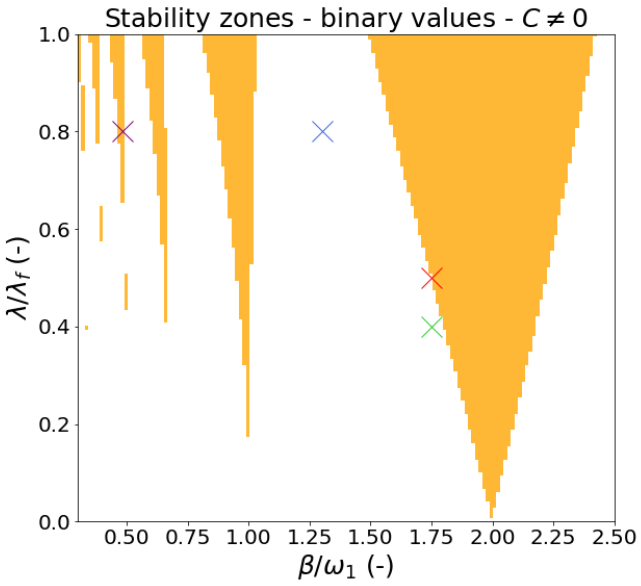

Figure 10: Instability tongues in the undamped linear case with $\eta = 0$. Instability is showed in orange while stability is represented in white. The highlighted points are points we will look at in the following to have some insight on dynamic behavior.

We observe that instability takes shape of tongues that expand as we go towards increasing λ. Then, the more we load the more unstable the structure is, except pulsation plays as well an important role.

We indeed note a finite number of these tongues, each representing a resonance point. By association, we have stable positions (white zones).

Graph 12 helps generalizing our study and displaying multiple parameters at once. We thereby observe same behaviors than detailed in section 3, for an undamped system.

In order to conclude on our stability analysis, we will now go through some points of the graph to confirm we now understand stability of the system.

Highlighted points

In this part we show dynamic behavior of the 4 highlighted points in Floquet instability tongues graph 12:

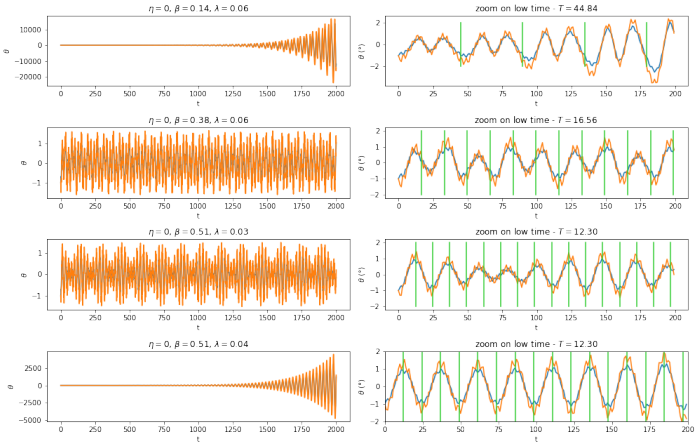

Figure 11: Highlighted points in figure 12. Vertical green bars are meant to split signal in terms of period. **Then, we are in same loading state every period.**

In graph 11 we show the dynamic behavior of the two bars depending on where one stands in Floquet graph 12. We confirm that stability depends on time at which we perturbate system and amplitude considered.

Comparing 2 first graphs of 11 with each others we see that at a constant loading (constant value, still time-dependent), the timing at which we load matters a lot. Then, it looks like if one stimulates system when θ_α is at a maximum, the system will most likely present flutter and eventually be unstable.

On the other hand, comparing the two last graphs of 11, it comes that the force as well plays an important part. Then, the more we load structure (i.e. the higher λ is), the more structure is unstable. In addition to timing there is therefore the fact that the bigger the load the more energy we provide to the structure and potentially the less it can handle, resulting in an unstable behavior.

We note that graph 12 presents only a part of the possible points one can consider. If we extend this graph to higher load, it appears that stable states still exist in the middle of more and more unstable cases. The point is to note that there theoretically always is a stable state, provided one parametrizes system at good time B.

Eventually, these results would be helped by experimental observations. With confirmation of well doing of our analysis, it would then be possible for one to work actively (as opposed to passive approach here) on the system by trying to change stimulation during motion, thereby provoking or preventing instability at choice.

Conclusion & Perspectives

This paper allowed us to study the behaviour of the dynamic system's stability: the Ziegler column, in particular in the context of aircraft design. The aim then was to characterise the loading conditions under which low frequency resonance can be avoided.
A first loading mode was studied corresponding to a constant conservative force, i.e. with constant direction. The study of stability around the natural equilibrium position showed the existence of a critical load: the first critical buckling load at $\lambda = 0.072$, below which the system remains stable and above which there is a bifurcation and the structure tends towards a new equilibrium outside its initial position. This part introduced the possibility of a first type of instability.

The second type of loading corresponded to a follower force: the direction of the force remains collinear to the second bar. Again, a critical loading value appeared: the first critical friction load for a loading value $\lambda = 0.47$ (for zero damping). Beyond this force, the system maintains a oscillating motion despite the constant applied force. It can be seen that instability appears here at a higher force than in the first case. A following force is therefore less critical at first sight than a conservative force. This part highlighted the possibility of more than one physical explanation for instability.

Finally, the third type of loading was a periodic conservative force. A more thorough stability analysis had to be undertaken. Floquet's theory was then used. It was then observed that the stability depends on both the excitation pulsation of the force and the value of the amplitude of the force. A modal analysis shows that resonance frequencies exist for forces with a pulsation multiple of the natural frequencies of the structure. Coupled with the constraints on the amplitude of the force, we obtain stability tongues depending on the parameters of the structure.

This last part finally conclude on our problematic, as we now under which condition will the system be unstable at low amplitude (i.e. low λ). For one to prevent instability then it is necessary to damp oscillations actively or to have some physical insight to know well initialize system.

References

[1] A. Gonzalo, M.-M Cayetano, F. Oscar, G.-V Manuel. (2022). Fluid-structure interaction of multi-body systems: Methodology and applications. link document

[2] N. Arora, A. Hikaru, W. Shyy, A. Gupta (2018). Analysis of passive flexion in propelling a plunging plate using a torsion spring model. Journal of Fluid Mechanics, vol. 857, 562-604. doi:10.1017/jfm.2018.736 link document

[3] J. C. Chassaing. Course Lecture "Aeroelasticity" MU5MEF10, Sorbonne University, ∂'Alembert Institute, Sept, 2021.

[4] T. A. Weisshaar. Course Lecture "Aeroelasticity" AAE556, Purdue University, 2011. Chapter 2 Static aeroelasticity – structural loads and performance p. 93-100 downloadable link

[5] G. Floquet Sur les équations différentielles linéaires à coefficients périodiques. Annales scientifiques de l'École Normale Supérieure, Série 2, Tome 12 (1883), pp. 47-88. doi : 10.24033/asens.220. downloadable link

A Matricial system

As we study dynamical system 1 we can use the usual matricial representation, with F_{NL} term accounting for a part of system's non-linearities:

$$\underline{\underline{M}}.\underline{\ddot{\theta}} + \underline{\underline{C}}.\underline{\dot{\theta}} + \underline{\underline{K}}.\underline{\theta} + \underline{F}_{NL} = \underline{0}$$

$$\underline{\underline{M}} = \begin{bmatrix} 1 & \frac{3}{8}c_{1-2} \\ \frac{3}{2}c_{1-2} & 1 \end{bmatrix}; \qquad \underline{\underline{C}} = \begin{bmatrix} 1 & -1/2 \\ -2 & 2 \end{bmatrix} . \frac{1}{Q};$$

$$\underline{\underline{K}} = \begin{bmatrix} 3/8 & -3/16 \\ -3/4 & 3/4 \end{bmatrix} . \frac{1}{Q};$$

$$\underline{F}_{NL} = \begin{bmatrix} 3/8.\dot{\theta}_2.s_{1-2} + \lambda.c_{\beta.\tau}\left[c_1.s_{\eta 2} - s_1.c_{\eta 2}\right] \\ -3/2.\dot{\theta}_1.s_{1-2} + 4\lambda.c_{\beta.\tau}\left[c_2.s_{\eta 2} - s_2.c_{\eta 2}\right] \end{bmatrix};$$

with $c, s_{1-2} = cos, sin(\theta_1 - \theta_2)$; $c, s_{\eta 2} = cos, sin(\eta\theta_2)$. By setting $\underline{y} = {}^{t}[\theta_1, \theta_2, \dot{\theta}_1, \dot{\theta}_2]$ we then get differential matricial system $\dot{\underline{y}} = \underline{\underline{J}}.\underline{y} + \underline{F}_{NL}$.

B Extension Floquet instability tongue graph

In this last appendix, we provide a graph giving an idea of a more general stability theory where one can see the interaction between load and pulsation is more complex than the way it's been tackled throughout this paper:

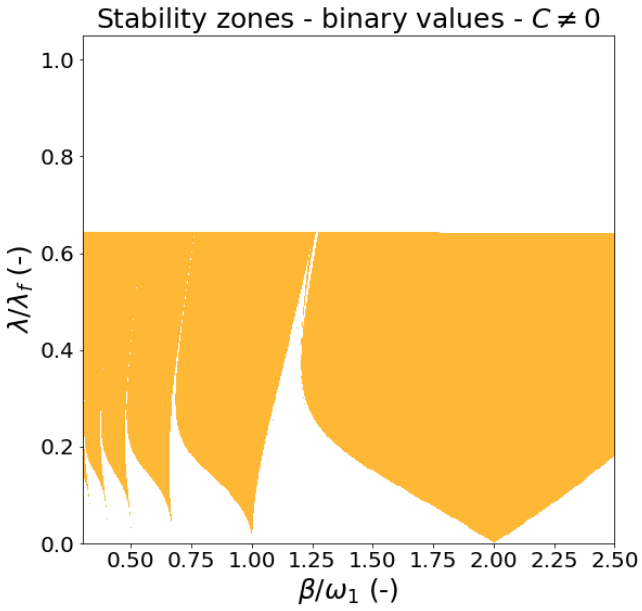

Figure 12: Instability tongues in the undamped linear case with $\eta = 0$. This graph is an extension of graph 12

Note that upper part (above $\lambda \approx 0.6$) exists but has not been plotted due to long calculation time.